

EFFECT OF SAMPLE MASS ON THE KINETICS OF THERMAL DECOMPOSITION OF A SOLID

II. Isothermal dehydration of $\text{Li}_2\text{SO}_4 \cdot \text{H}_2\text{O}$

N. Koga and H. Tanaka

CHEMISTRY LABORATORY, FACULTY OF SCHOOL EDUCATION, HIROSHIMA UNIVERSITY, 3-1-33 SHINONOME, MINAMI-KU, HIROSHIMA, 734 JAPAN

Effects of sample mass on the kinetics of isothermal dehydration of crushed crystals of $\text{Li}_2\text{SO}_4 \cdot \text{H}_2\text{O}$ were investigated using conventional TG. The process was characterized by a combination of Avrami-Erofeyev and contracting geometry models. Distribution of the fractional reaction, α , in particles within the sample assembly as well as the change in the rate of gross diffusion of the evolved water vapour appear responsible for the sample-mass-dependent kinetic parameters obtained for the system.

Keywords: effect of sample mass, isothermal dehydration, kinetics, $\text{Li}_2\text{SO}_4 \cdot \text{H}_2\text{O}$

Introduction

Experimental evidence shows that the overall kinetics of thermal decomposition of solids depends largely on the sample and experimental conditions [1, 2] when conventional thermoanalytical (TA) techniques are employed in kinetic evaluation of the process. Sample mass is one such experimental variable, which affects the reaction temperature region and shape of the TA curves [3–5]. The sample-mass-dependence of kinetic parameters has been investigated by many authors [6–11]. For best results, it has been recommended that kinetics are studied under moderate reaction conditions using a small sample size to reduce gradients in temperature and pressure [12]. From this viewpoint controlled transformation rate thermal analysis (CRTA) [13] and/or quasi-isobaric quasi-isothermal thermal analysis (QQTA) [14] have the merit of retaining the self-generated reaction condition constant during the reaction. On the other hand, some investigators have proposed extrapolating the kinetic parameters to mass zero using empirical linear relationships between kinetic parameters and sample mass [6, 9]. These studies indicate that variation in apparent kinetic parameters depending on sample mass results from difficulty in obtaining TA curves under ideal conditions – an inherent problem in kinetic evaluation of TA curves. This problem is also

connected with introduction of the fractional reaction, α , into the kinetic description based on the physico-geometric feature of the solid-state reaction [15, 16].

In the present study, the sample mass-dependence of the kinetic parameters is tentatively explained by taking into account the physico-chemical meaning of the kinetic curves obtained by conventional TG and the applicability of kinetic description based on the physico-chemical models for the experimental TG curves. Isothermal dehydration of crushed crystals of lithium sulphate monohydrate was selected as a model reaction.

Experimental

Single crystals of $\text{Li}_2\text{SO}_4 \cdot \text{H}_2\text{O}$ were grown from a supersaturated aqueous solution at room temperature. The crushed crystals were obtained by grinding single crystals with a mortar and pestle and collecting a sieved 100 to 170 mesh fraction. The sample was characterized by TG and IR, and stored before rate studies for about three weeks to avoid effects of ageing on the kinetics. Sample sizes nominally controlled were 2.5, 5.0, 7.5, 10.0, 15.0, 20.0 and 25.0 mg, material being packed by light tapping into a cylindrical platinum crucible 5 mm in diameter and 2.5 mm high. The isothermal mass-loss traces were recorded using a Shimadzu TGA-50 instrument at various constant temperatures of 79°–100°C, under nitrogen flowing at 30 ml/min.

Results and discussion

Figure 1 shows the effect of sample mass on the fractional reaction, α , vs. time, t , plot for the isothermal dehydration of the salt at 91°C. It can be seen that the α - t curve shifts along the time-coordinate with increasing sample mass. Although there is microscopic evidence that the reaction proceeds geometrically by volume contraction of the reactant particle with spherical symmetry [17–19], such a shift cannot be rationalized from the contracting-volume-based kinetic expression. Change in self-generated atmospheric conditions with sample mass, accompanied by variation in gross diffusion rate of evolved vapour, could be one of the causes of the discrepancy between kinetic curves and physico-geometry-based kinetic description [20]. The temperature gradient within the sample matrix due to self-cooling effects should also be taken into account [21]. A systematic distribution in α value in particles within the sample matrix seems to occur during the early stage of reaction [22]. The consequent kinetic process then can be recognized apparently as in the case of reaction with the particle size distribution [23].

Plots of overall rate of conversion, $d\alpha/dt$, against α are shown in Fig. 2. The value of $d\alpha/dt$ is apparently sample-mass-dependent, as would be expected from Fig. 1. Each overall reaction rate, accelerated initially, is approximately constant in the range $0.1 < \alpha < 0.5$ followed by the deceleration stage in $\alpha > 0.5$. The process

has been characterized formally by a combination of an Avrami-Erofeyev model, A_m , which is representative of the earlier stages, with a contracting geometry model, R_n , which becomes predominant as the reaction proceeds [17].

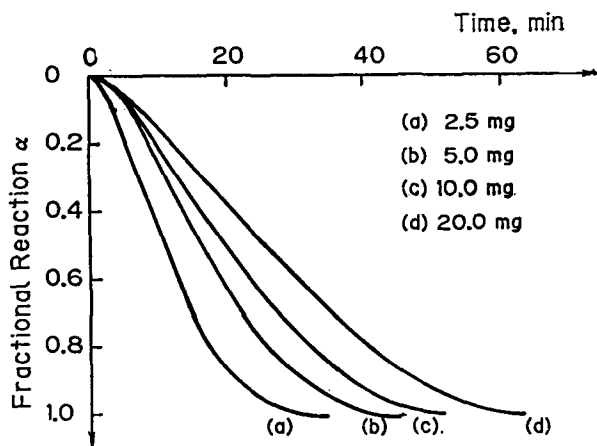


Fig. 1 Effect of sample mass on the α vs. t curve for isothermal dehydration of crushed crystals of $\text{Li}_2\text{SO}_4 \cdot \text{H}_2\text{O}$ (-100+170 mesh)

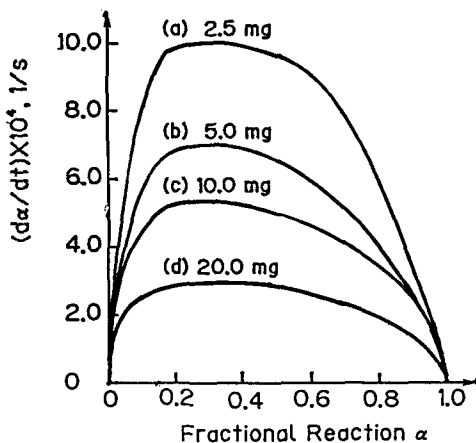


Fig. 2 Effect of sample mass on $d\alpha/dt$ vs. α curve for isothermal dehydration of crushed crystals of $\text{Li}_2\text{SO}_4 \cdot \text{H}_2\text{O}$ (-100+170 mesh)

The formal obedience of the kinetic curve to physico-geometrical models was estimated through the plots of possible function $F(\alpha)$ against t in the respective α range of kinetic characteristics. In the earlier stages of reaction ($0.1 < \alpha < 0.5$) ex-

cellent linearity of the $F(\alpha)$ - t plot was obtained in terms of both the R_n ($n = 1$) and A_m ($1 < m < 2$) models. Varying the exponent of n and m continuously, the non-integral values were estimated, which are the parameters fixed mathematically to yield the highest correlation coefficient γ [24]. Table 1 lists the appropriate values of n and m for different sample sizes, together with the apparent rate constant k_{app} and γ at 91°C. It is seen from Table 1 that the values of n and m are nearly constant and independent of sample mass. The value of k_{app} decreases with increasing sample mass. Such a change in the value of k_{app} cannot be explained by assuming nucleation and growth models, such as an A_m law. On the other hand, obedience to the R_1 law is supported by the approximate constant rate of weight-loss within the restricted range of $0.1 < \alpha < 0.5$ (Fig. 2). In this case, the kinetics are not treated in terms of the physico-geometric description of the reaction, but in terms of the overall description on the weight-loss process of the sample matrix, being interpreted as in the case of evaporation from a liquid surface.

Table 1 Appropriate values of n and m in the R_n and A_m laws estimated within $0.1 < \alpha < 0.5$, together with the apparent rate constant k_{app} and correlation coefficient γ at 91°C

| Sample mass / mg | $R_n = 1 - (1 - \alpha)^{1/n} = k_{app}t$ | | | $A_m = [-\ln(1 - \alpha)]^{1/m} = k_{app}t$ | | |
|---------------------|---|--------------------------------|----------|---|--------------------------------|----------|
| | n | $k_{app} \times 10^4 / s^{-1}$ | γ | m | $k_{app} \times 10^4 / s^{-1}$ | γ |
| 2.5 | 1.1 | 7.20 | 0.9997 | 1.6 | 10.34 | 0.9996 |
| 5.0 | 1.0 | 6.29 | 0.9999 | 1.6 | 8.69 | 0.9999 |
| 7.5 | 1.0 | 5.86 | 0.9999 | 1.6 | 8.12 | 0.9998 |
| 10.0 | 1.0 | 4.90 | 0.9998 | 1.6 | 6.71 | 0.9999 |
| 15.0 | 1.0 | 3.80 | 0.9999 | 1.6 | 5.16 | 0.9999 |
| 20.0 | 1.0 | 3.68 | 0.9999 | 1.6 | 5.04 | 0.9999 |
| 25.0 | 1.0 | 3.27 | 0.9999 | 1.6 | 4.46 | 0.9999 |

Sample-mass-dependent variation in k_{app} is a possible cause of the sample-mass-dependent Arrhenius parameters, being related to the linear interdependence of these parameters, i.e. kinetic compensation effect [25–27]. The sample-mass-dependence of k_{app} is reflected directly by the value of A_{app} , resulting in a slight but detectable change in E_{app} [28]. Simply, the relationship between k_{app} and sample mass, m_o , is represented by the following equation [16, 28],

$$k_{app} = \frac{kSp}{m_o} \quad (1)$$

where k is the rate of reaction interface advancement, S is the area of the reaction interface, and ρ is the volume density of the sample matrix. Figure 3 shows the plots of k_{app} vs. m_o^{-1} within the range $0.1 < \alpha < 0.5$ at various temperatures. The plots show a fairly linear relationship with a slope of kSp , which is a sample-

mass-independent rate constant. Such a specific rate constant is useful for obtaining the more reliable Arrhenius parameters [16, 28], because the sample-mass-dependence of the A_{app} value is masked, yielding a unique value of E_{app} . Figure 4 shows the plot of $\ln kSp$ against reciprocal temperature, T^{-1} . The apparent Arrhenius parameters thus calculated are $E_{app} = 98.1 \pm 1.9$ kJ/mol and $\log A_{app} = 11.3 \pm 0.3$ 1/s, with $\gamma = -0.9939$.

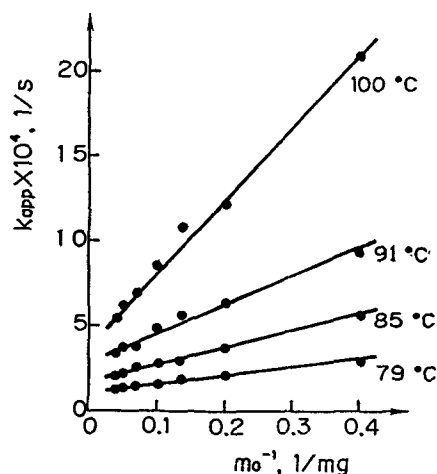


Fig. 3 Typical plots of apparent rate constant k_{app} against reciprocal sample mass m_0^{-1} in a restricted range of $0.1 < \alpha < 0.5$

Table 2 Appropriate value of n in the R_n law, within the restricted range of $0.5 < \alpha < 0.9$, together with the values of k_{app} and γ at 91°C

| Sample mass /mg | n | $k_{app} \times 10^4 /s^{-1}$ | γ |
|-----------------|-----|-------------------------------|----------|
| 2.5 | 2.7 | 4.97 | 0.9999 |
| 5.0 | 2.2 | 4.07 | 0.9999 |
| 7.5 | 2.1 | 3.88 | 0.9999 |
| 10.0 | 1.9 | 3.54 | 0.9999 |
| 15.0 | 1.8 | 2.80 | 0.9999 |
| 20.0 | 1.7 | 2.77 | 0.9999 |
| 25.0 | 1.7 | 2.67 | 0.9998 |

The later stage of reaction, $0.5 < \alpha < 0.9$, was well described by the R_n law, irrespective of the sample mass examined. Table 2 lists the most appropriate non-integral values of n , together with values of k_{app} and γ at 91°C. It is worth noting that the n value decreases with increasing sample mass, although the n value is constant within the restricted range of $0.1 < \alpha < 0.5$. In contrast to the microscopic evidence of contracting cubes, the formal kinetic obedience to the R_n law, in

which n is not equal to 3, suggests that the TA curves do not necessary reflect the physico-geometric features of the reaction occurring in a particle of the sample assembly. The kinetic curves for the smaller sample mass show better correspondence to such a kinetic description. Variation in the value of n with increasing sample mass seems to be due to (i) change in the role of gross diffusion of evolved water vapour through the sample assembly [29, 30] and (ii) distribution in the fractional reaction of particles produced in the earlier stage [22]. The kinetic information obtained from such a TA curve has the overall character averaged over all the particles in the sample assembly.

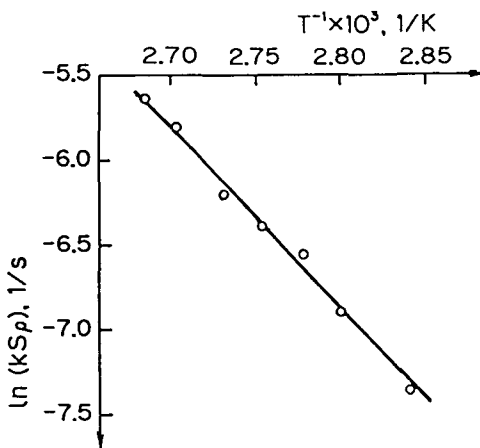


Fig. 4 Plot of $\ln(kSp)$ vs. reciprocal temperature T^{-1} in a restricted range of $0.1 < \alpha < 0.5$

In conclusion, the present study on the sample-mass-effect on the kinetics of isothermal dehydration of $\text{Li}_2\text{SO}_4 \cdot \text{H}_2\text{O}$ indicates that kinetic analysis of TA curves should be made using the mathematical description corresponding physically to the kinetic information of the TA curves. An empirical curve-fitting method based on a kinetic description does not necessary provide meaningful kinetic results.

* * *

The authors thank H. Takemoto for his assistance in the experimental part of this work.

References

- 1 J. Šestak, *Thermophysical Properties of Solids*, Elsevier, Amsterdam, 1984.
- 2 N. Koga, Ph. D. Thesis, Inst. Chem. Technol. Pardubice (CSFR), 1991.
- 3 J. Simon, *J. Thermal Anal.*, 5 (1973) 271.
- 4 T. Székely, G. Várhegyi, F. Till, P. Szabó and E. Jakab, *J. Anal. Appl. Prol.*, 11 (1987) 71; 83.

- 5 G. Várhegyi, T. Székely, F. Till, E. Jakab and P. Szabó, *J. Thermal Anal.*, 33 (1988) 87.
- 6 T. B. Flanagan, J. W. Simons and P. M. Fichte, *Chem. Commun.*, (1971) 370.
- 7 P. K. Gallagher and D. W. Johnson, *Thermochim. Acta*, 6 (1973) 67.
- 8 G. G. T. Guarini, R. Spinicci, F. M. Carlini and D. Donati, *J. Thermal Anal.*, 5 (1973) 307.
- 9 K. N. Ninan, *Thermochim. Acta*, 74 (1984) 143.
- 10 H. Tanaka and H. Takemoto, *J. Thermal Anal.*, 38 (1992) 429.
- 11 H. Tanaka, N. Koga and J. Šestak, *Thermochim. Acta*, 203 (1992) 203.
- 12 M. Reading, D. Dollimore, J. Rouquerol and F. Rouquerol, *J. Thermal Anal.*, 29 (1984) 775.
- 13 J. Rouquerol, *J. Thermal Anal.*, 5 (1973) 203.
- 14 J. Paulik and F. Paulik, *Anal. Chim. Acta*, 56 (1971) 328.
- 15 D. Fatu and E. Segal, *Thermochim. Acta*, 55 (1982) 351; 111 (1987) 349.
- 16 N. Koga, H. Tanaka and J. Šestak, *J. Thermal Anal.*, 38 (1992) 2553.
- 17 N. Koga and H. Tanaka, *J. Phys. Chem.*, 93 (1989) 7793.
- 18 A. K. Galwey, N. Koga and H. Tanaka, *J. Chem. Soc. Faraday Trans.*, 86 (1990) 531.
- 19 N. Koga and H. Tanaka, *Thermochim. Acta*, 185 (1991) 135.
- 20 N. Koga and H. Tanaka, *Thermochim. Acta*, 183 (1991) 125.
- 21 H. Tanaka and N. Koga, *J. Thermal Anal.*, 36 (1990) 2601.
- 22 H. Tanaka and N. Koga, *Thermochim. Acta*, 163 (1990) 295.
- 23 G. A. Urrutia and M. A. Blesa, *React. Solids*, 6 (1988) 281.
- 24 G. D. Anthony and P. D. Garn, *J. Am. Ceram. Soc.*, 57 (1974) 132.
- 25 N. Koga and J. Šestak, *Thermochim. Acta*, 182 (1991) 201.
- 26 N. Koga and H. Tanaka, *J. Thermal Anal.*, 37 (1991) 347.
- 27 N. Koga and J. Šestak, *J. Thermal Anal.*, 37 (1991) 1103.
- 28 N. Koga and H. Tanaka, *Thermochim. Acta*, 209 (1992) 127.
- 29 H. Tanaka and N. Koga, *Thermochim. Acta*, 173 (1990) 53.
- 30 N. Koga and H. Tanaka, *Solid State Ionics*, 44 (1990) 1.

Zusammenfassung — Mittels herkömmlicher TG wurde der Einfluß der Probenmasse auf die Kinetik der isothermen Dehydratation zerkleinerter Kristalle von $\text{Li}_2\text{SO}_4 \cdot \text{H}_2\text{O}$ untersucht. Der Prozeß wird durch eine Kombination des Avrami-Erofeyev und des Kontraktionsgeometrie-modelles charakterisiert. Der Beitrag der Teilreaktion in Partikeln innerhalb der Probe als auch die Änderung der Bruttodiffusionsgeschwindigkeit des freigesetzten Wasserdampfes erscheinen für die probenmassenabhängigen kinetischen Parameter des Systemes verantwortlich zu sein.